*29th EPS Conference on Plasma Phys. and Contr. Fusion Montreux, 17-21 June 2002 ECA Vol. **26B**, O-2.08 (2002)*

Demonstration of the ITER Ignition Figure of Merit at $q_{95} > 4$ in Stationary Plasmas in DIII–D

M.R. Wade,[1] T.C. Luce,[2] P.A. Politzer,[2] J.R. Ferron,[2] A.W. Hyatt,[2]
J.T. Scoville,[2] R.J. La Haye,[2] J.E. Kinsey,[3] C.J. Lasnier,[4] M. Murakami,[1] C.C. Petty[2]

[1]Oak Ridge National Laboratory, Oak Ridge, Tennessee, 37831 USA
email: wade@fusion.gat.com
[2]General Atomics, P.O. Box 85608, San Diego, California, 92186-5608 USA
[3]Lehigh University, Bethlehem, Pennsylvania 18015 USA
[4]Lawrence Livermore National Laboratory, P.O. Box 808, Livermore, California 94551 USA

In order to maximize the probability of achieving ignition, the present International Thermonuclear Experimental Reactor (ITER) [1] design (as well as many of its predecessors) is based on operation at high plasma current. This constraint poses many significant engineering challenges, primarily related to the possibility of a sudden termination of the plasma current. Currents induced in the vessel and associated systems in such an event can lead to large forces, and runaway electrons may cause damage to the interior of the vacuum vessel. Present design methods (including those used for ITER) assume that the probability of experiencing such a major disruption increases with plasma current at fixed magnetic field and size. Because fusion performance is assumed to scale in a similar manner, reactor designs tend to seek a compromise between increased fusion performance and reduced susceptibility to disruptions, generally resulting in a design with $q_{95} \sim 3.0$. Discharges recently developed in the DIII–D tokamak offer a way to obtain equilvalent fusion performance with more margin against disruption consequences, having obtained an ignition figure of merit comparable to the ITER baseline scenario with $q_{95} = 4.5$. These discharges have been shown to be stationary on the thermal, resistive, and wall time scales and involve feedback control only of global quantities rather than profiles.

The temporal evolution of an example of this class of discharges is shown in Fig. 1. Neutral beam injection (NBI) is initiated early in the current ramp [Fig. 1(a)]. L–mode is maintained throughout this phase by using a magnetic configuration with the dominant (upper) X–point opposite from the ion ∇B drift direction, thereby increasing the L-H transition power threshold. Sufficient NBI power is used to reduce the current penetration such that $q_{\min} > 1$ at the end of the current ramp without inducing an internal transport barrier. At the end of the current ramp, an L-H transition is induced by transiently changing the plasma shape to a symmetric double-null shape. After the transition, the plasma shape is returned to a slightly unbalanced double-null shape with the dominant X–point being the upper divertor. This facilitates density control using the optimized divertor baffling and cryo-pumps in the upper divertor of DIII–D [2]. Regulation of the density subsequent to the L-H transition is accomplished via feedback control using gas injection. During the stationary phase, the plasma stored energy

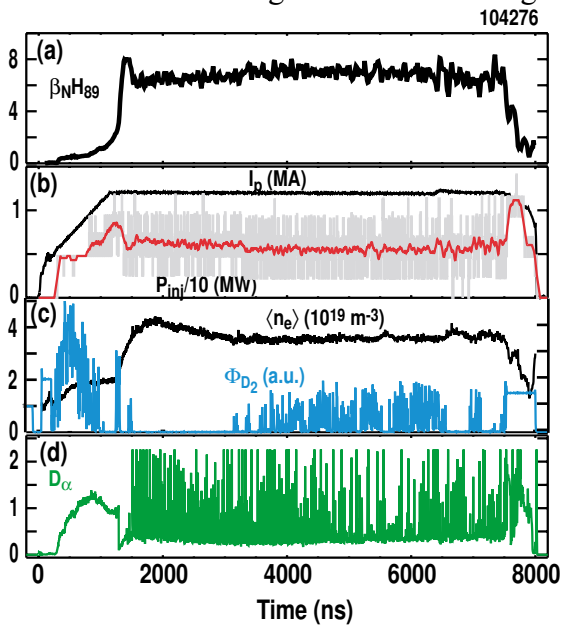

Fig. 1. Plasma parameters versus time for a discharge (104276) with $\beta_N H_{89} \sim 7$ for 35 τ_E: (a) $\beta_N H_{89}$; (b) Plasma current (MA), neutral beam injected power (10 MW); (c) line-averaged density (10^{19} m^{-3}), gas injection rate (a.u.), (d) divertor D_α (a.u.).

is also controlled via feedback control of the NBI power, with the average NBI power in this case being ~ 6.0 MW. After ~ 2 s, the current profile becomes stationary, consistent with the estimated current profile relaxation time of 1.8 s. Reconstructions of the magnetic equilibrium using the MSE data indicate that the profile of the safety factor (q) is monotonic and has $q(0) \sim 1.05$. No sawtooth or fishbone instabilities are observed. An m=3/n=2 tearing mode is triggered at 2.0 s, which then persists throughout the remainder of the discharge albeit at a small amplitude (~ 3 G measured at the wall). Although the temporal behavior of this mode is similar to that expected for a neoclassical tearing mode, the seeding mechanism for this tearing mode is still unknown. The reduction in confinement due to this mode is relatively small (<10%) and the confinement quality remains good ($H_{89p} \sim 2.5$). Global particle balance measurements also indicate that the wall comes into equilibrium (i.e., $dN_{wall}/dt = 0$) within 1 s of the beginning of high power phase. This balance is achieved through tight coupling of the divertor plasma to the two upper divertor pumps in DIII–D. In fact, the particle exhaust efficiency is of such good quality that gas puffing is required to maintain a constant line-averaged density ($n_e = 3.5 \times 10^{19}$ m^{-3} = 0.3 n_{GW}).

The discharge shown in Fig. 1 sustained normalized fusion performance ($\beta_N H_{89}$)~ 7 for ~ 35 energy confinement times (τ_E) and is terminated by hardware limitations, not by evolution of the plasma profiles or plasma instabilities. Here, β_N is normalized β defined as $\beta_N = \beta/(I/aB)$, where I is the plasma current (MA), a in the minor radius (m) and B is the toroidal field (T) and H_{89} is the energy confinement time relative to the ITER L–mode energy confinement scaling. In other cases, $\beta_N H_{89} \sim 8.5$ has been achieved for ~4 τ_E, again only limited by hardware limitations. A comparison of several performance measures of these discharges with a conventional, $q_{95} \sim 3.0$, ELMing H–mode discharge is shown in Table 1. The low q_{95} discharge has $\beta_N H_{89}$ ~5 for ~ 4 τ_E, but is terminated by a disruption caused by a rotating m=2/n=1 tearing mode which locked. Although no optimization has been done in this case, it is likely that the performance will need to be reduced to achieve steady operation. The measures of performance compared in Table 1 include β_N, $\beta_N H_{89}$, and the ignition figure of merit $\left(\beta_N H_{89}/q_{95}^2\right)$ which is generally used as a relative measure of the achievable $\beta\tau$. Significant improvements in both β_N and $\beta_N H_{89}$ are obtained in the best of the high q_{95} cases relative to the $q_{95} = 3.0$ case. Furthermore, even with the 50% increase in q_{95}, the ignition figure of merit in the best high q_{95} case is nearly equivalent to that achieved in the $q_{95} = 3.0$ case. In all cases, the present discharges at higher q_{95} have the ignition figure of merit at or above the nominal ITER level.

This improvement in performance is ascribed to both improvements in stability and transport in these discharges. From a stability point-of-view, stationary operation at $\beta_N > 3.0$ is made possible by the absence of seeding events for neoclassical tearing modes (NTMs) such as sawteeth or fishbones. The absence of these internal modes, generally associated with $q(0)$ very close or below unity, appears to be due to the establishment of a stationary current density profile with $q(0) > 1$. Because of the tendency for the Ohmic current to peak strongly on-axis, this stationary state with $q(0) > 1$ can only be established by the explusion of

Table 1

	ITER	$q_{95} > 4.0$*		DIII–D Reference
		Best	Routine	
q_{95}	3.0	4.4	4.3	3.0
β_N	1.8	3.2	2.7	2.7
$\beta_N H_{89}$	3.6	8.5	7.0	5.0
$\left(\beta_N H_{89}/q_{95}^2\right)$	0.4	0.44	0.38	0.55
τ_E/τ_{dur}	> 300	4	35	~ 4

*Simultaneously achieved

current (or magnetic flux) through some non-diffusive process. Analysis of the internal loop voltage using the VLOOP analysis code [3] through time histories of magnetic reconstructions indicates an apparent voltage source of ~5 mV near the location of the aforementioned m=3/n=2 tearing mode. It is conjectured that through a dynamo-like process, this mode is maintaining the $\Delta V_{\phi,eff}$, which helps to keep $q(0) > 1$. The "dynamo" appears as a difference in RE_ϕ because the equilibrium analysis assumes axisymmetry and thus has no other way to account for the $\langle v \times B \rangle$ associated with the non-axisymmetric mode.

From a transport point-of-view, transport analysis indicates that the single-fluid diffusivity χ_{eff} in the high q_{95} cases is comparable to the q_{95} = 3.0 case [see Fig. 2(a)] even though q is significantly higher over much of the profile. This is a significant improvement over the expected level based either on global confinement scaling in which $\chi_{eff} \sim q^{-1.4}$ or local transport scaling from nondimensionsal scaling studies in which $\chi_{eff} \sim q^{-2.0}$ [4]. The observed T_e and T_i profiles in the high q_{95} case are well matched by GLF23 transport model simulations [5] [see Fig. 2(b)]. This model is a gyrofluid representation of the transport due to ion temperature (ITG), trapped electron modes, and electron temperature gradient (ETG) modes and includes the effect of E×B on shear on the mode spectrum. For this calculation, the experimental values at ρ = 0.85 are used as boundary conditions and the experimental density is input as well as model calculations of the heat sources. Detailed analysis of the simulations indicate that the improvement in transport is due to a combination of high T_i/T_e and sufficient E×B shear acting to maintain low levels of turbulence. However, the simulations indicate that turbulence is not completely suppressed, which is consistent with χ_i being significantly higher than the neoclassical prediction χ_i^{neo}.

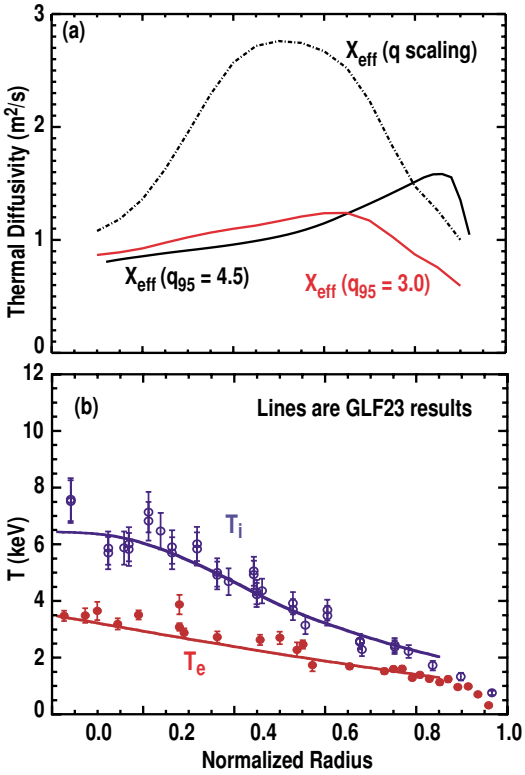

Fig. 2. (a) Comparison of the single fluid diffusivity χ_{eff} for the discharge in Fig. 1 at 5.7 s (black), χ_{eff} in the q_{95} = 3.0 reference discharge (red), and χ_{eff} scaled from the q_{95} case assuming $\chi_{eff} \propto q$; (b) comparsion of the measured electron (closed circles) and ion (open circles) temperature profiles versus drift-wave model predictions for ion (solid line) and electron (dashed line) temperatures.

Projecting these discharges to burning plasmas, one finds that $\beta_N H_{89}/q_{95}^2$ in the best case ($\beta_N H_{89}$ = 8.5 at q_{95} = 4.5) is comparable to that in the ITER baseline scenario ($\beta_N H_{89}$ = 3.6 at q_{95} = 3.0). The main advantage of operation at higher q_{95} lies in the reduction in plasma current. Depending on the type of disruption, the forces on the vessel and support structure as well as the generated runaway electron current should be reduced by 30%–50%.

Preliminary studies exploring the operating space over which high performance conditions at high q_{95} can be established and maintained indicate that the available operation space is quite large. Because a primary concern regarding these discharges is the relatively low density and high T_i/T_e, experiments have been conducted exploring higher density operation. Representative figures of merit including τ_E, ion collisionality ν_{*i}, Z_{eff}, and T_i/T_e are shown in Fig. 3 for a density scan ranging from n_{GW} = 0.3–0.5. Over this range of density, confinement quality is observed to decrease only slightly while ν_{*i}, Z_{eff}, and T_i/T_e move much closer to the ITER design values for these parameters. In particular, the trends seen in Fig. 3 indicate that by increasing the density to n_{GW} = 0.7, collisionality and T_i/T_e

values consistent with ITER should be achievable. Separate studies have also shown that high normalized performance can be obtained with q_{95} as low as 3.5. $\beta_N H_{89}/q_{95}^2$ in this case is nearly the same as achieved in the conventional, q_{95} = 3.0 case.

The operational limit in these discharges appears to be the onset of m=2, n=1 (2/1) NTMs. Because the classical NTM seed mechanisms (e.g., sawteeth, fishbones) are not present in these discharges, it is believed that that these discharges can operate robustly at much higher β_N than conventional, sawtoothing, ELMing H–mode discharges. Experi-mentally, it has been shown that these discharges can be operated at the no-wall ideal, β limit. An example of this is shown in Fig. 4 in which β_N is slowly ramped up to 4 ℓ_i, which is representative of the no-wall β limit in these discharges. β_N~3.2 is achieved with little change in confinement quality (H_{89}~2.6) or plasma rotation observed. Efforts at increasing β early in the discharge evolution (< 3.5 s) have generally been unsuccessful with m=2, n=1 NTMs occurring between 3.0 and 4.0 s as $q(0)$ approaches unity. Empirically, the presence of a robust m=3, n=2 NTM is also favorable in avoiding the m=2, n=1 NTM onset. Recent experiments in these types of discharges have also shown that the 2/1 NTMs can be stabilized through the use of electron cyclotron current drive (ECCD) near the q = 2 surface. Future experiments will seek to stabilize or suppress the 2/1 NTM entirely using ECCD.

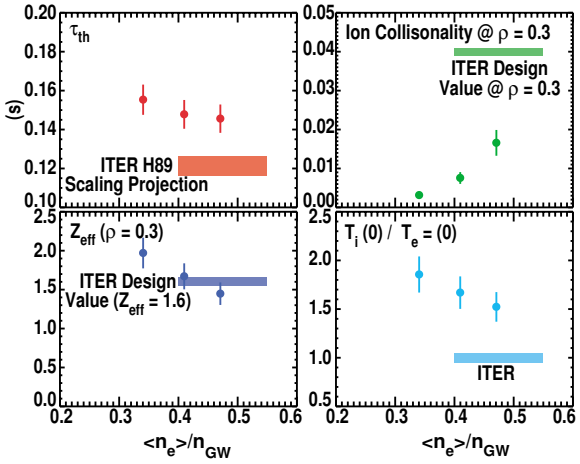

Fig. 3. Dependence of the energy confinement time τ_{th}, ion collisionality ν^*_i, Z_{eff}, and T_i/T_e on density in stationary, high performance discharges.

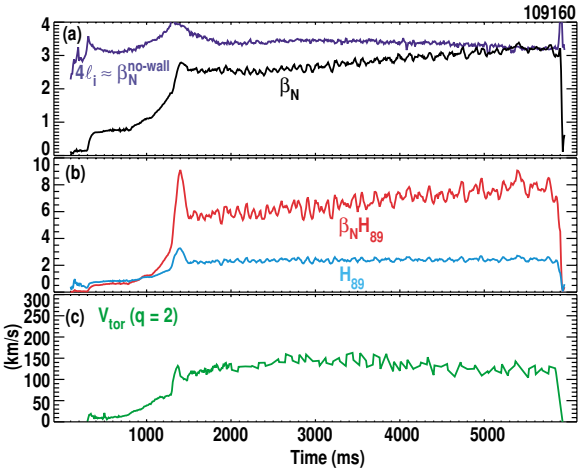

Fig. 4. Plasma parameters versus time for a discharge (109160) which achieves $\beta_N \sim \beta_N^{no\text{-}wall}$: (a) β_N (lower curve) and 4 ℓ_i (upper curve); (b) $\beta_N H_{89}$ (upper curve) and H_{89} (lower curve); and (c) toroidal rotation near the q= 2 surface. Hardware constraints cause trip at 5.8 s.

In conclusion, a stationary scenario with significant benefits for a burning plasma experiment has been demonstrated in the DIII–D tokamak. Normalized performance ($\beta_N H_{89}$) has reached 7.0 for 35 τ_E and 8.5 for 4 τ_E, both limited by hardware. This level of performance approaches that of the standard low-q ELMing H–mode scenario envisioned for ITER and other burning plasma experiments. The advance in normalized performance is due both to higher β_N and higher H_{89} than that anticipated for low-q ELMing H–mode.

Work supported by U.S. Department of Energy under Contracts DE-AC05-00OR22725, DE-AC03-99ER54463, W-7405-ENG-48, and DE-AC04-94AL85000.

[1] ITER Physics Basis Editors et al., Nucl Fusion **39** 2137 (1999).
[2] M.A. Mahdavi et al., J. Nucl. Mater. **290-293** 905 (2001).
[3] C.B. Forest et al., Phys. Rev. Lett. **73** 2444 (1994).
[4] C.C. Petty et al., Phys. Plasmas **5** 1695 (1998).
[5] R.E. Waltz et al., Phys. Plasmas **5** 1784 (1998).